

SUPPORTING INFORMATION

Surface characterisation of phosphine and phosphite stabilised Rh nanoparticles: a model study.

Jessica Llop Castelbou^a, Pascal Blondeau^b, Carmen Claver^{a*} and Cyril Godard^{a*}

^aDepartament de Química Física I Inorgànica, Universitat Rovira I Virgili, C/ Marcel·li Domingo s/n, Campus Sescelades, 43007, Tarragona, Spain. Fax: (+34) 977 559563, E-mail: cyril.godard@urv.cat

^bDepartament de Química Analítica i Orgànica, Universitat Rovira I Virgili, C/ Marcel·li Domingo s/n, Campus Sescelades, 43007, Tarragona, Spain.

Table of contents :

S1. General, materials and characterization techniques.

S2. Synthesis of Rhodium $[\text{Rh}(\eta^3\text{-C}_3\text{H}_5)_3]$ precursor from $\text{RhCl}_3 \cdot 3\text{H}_2\text{O}$

S3. Synthesis of rhodium nanoparticles stabilized by P-ligands

S4. Characterization of the rhodium nanoparticles Rh1-Rh2

S5. References

S1. General, materials and characterization techniques.

General methods. All syntheses were performed using standard Schlenk techniques under N₂ or Ar atmosphere. Chemicals were purchased from Aldrich Chemical Co, Fluka and Strem. All solvents were distilled over drying reagents and were deoxygenated before use. The precursor Rh(η^3 -(C₃H₅)₃), was prepared following previously described methods.^{[1][2]} The synthesis of Rh-nanoparticles were performed using 200 ml Fisher Porter and pressurized on a high pressure line.

The deuterated solvents for NMR measurements were dried over molecular sieves. ¹H, ¹³C {¹H}, and ³¹P {¹H} NMR spectra were obtained on a Varian Mercury 400 MHz spectrometer. Chemical shifts were calibrate relative to SiMe₄ (¹H and ¹³C NMR) as internal standard or 85 % H₃PO₄ as external standard (³¹P NMR).

The **TEM experiments** were performed at the “Unitat de Microscopia dels Serveis Científicotècnics de la Universitat Rovira I Virgili” (TEM-SCAN) in Tarragona with a Zeiss 10 CA electron microscope operating at 100 kV with resolution of 3 Å. The particles size distributions were determined by a manual analysis of enlarged images. At least 300 particles on a given grid were measured in order to obtain a statistical size distribution and a mean diameter.

XRD measurements were performed using a Siemens D5000 diffractometer (Bragg- Brentano parafocusing geometry and vertical θ - θ goniometer) fitted with a curved graphite diffracted- beam monochromator, incident and diffracted- beam Soller slits, a 0.06° receiving slit and scintillation counter as a detector. The angular 2θ diffraction range was between 26 and 95°. The data were collected with an angular step of 0.05° at 16s per step and sample rotation. A low background Si(510) wafer was used as sample holder. Cu_{k α} radiation was obtained from a copper X- ray tube operated at 40kV and 30mA.

WAXS analysis were performed at CEMES-CNRS. Samples were sealed in 1 mm diameter Lindemann glass capillaries. The samples were irradiated with graphite-monochromatized Moka (0.071069 nm) radiation and the X-ray intensity scattered measurements were performed using a dedicated two-axis diffractometer. Radial distribution functions (RDF) were obtained after Fourier transform of the reduced intensity functions.

The **TGA experiments** were carried out in the furnace of a Mettler Toledo TGA/SDTA851 instrument.

GS-MS analysis was carried out on a HP 6890A spectrometer, with an achiral HP-5 column (0.25mm x 30m x 0.25um), $T^a = 250^\circ\text{C}$ injector, flow 1.5ml/min.

XPS measurements were performed in a PHI 5500 Multitechnique System (from Physical Electronics) with a monochromatic X-ray source (Aluminium Kalfa line of 1486.6 eV energy and 350 W), placed perpendicular to the analyzer axis and calibrated using the 3d5/2 line of Ag with a full width at half maximum (FWHM) of 0.8 eV. The analyzed area was a circle of 0.8 mm diameter, and the selected resolution for the spectra was 187.5eV of Pass Energy and 0.8 eV/ step for the general spectra and 23.5 eV of Pass Energy and 0.1 eV/step for the spectra of the different elements in the depth profile spectra. A low energy electron gun (<10 eV) was used in order to discharge the surface when necessary. All measurements were performed in a ultra high vacuum (UHV) chamber pressure between 5×10^{-9} and 2×10^{-8} torr.

General procedure to perform hydrides titration

Each colloidal solution has been prepared in THF as previously described. On each fresh colloidal solution, five cycles of 1 minute vacuum/1 minute bubbling of argon were performed in order to eliminate the dihydrogen solved into the solvent. Then, 1 equivalent of the olefin (2-norbornene), previously filtered through alumina, were added. Samples were regularly taken from the solutions (after 24, 48 and 60 hours) for GC analyses and estimation of the olefins conversion into alkanes. The method used for the quantification of hydrides consists of 15min. at 40°C and a 3 ramp of $8^\circ\text{C}/\text{min}$. until 250°C .

To get nanoparticles- free solutions, filtration of the samples was realized through an Al_2O_3 pad. For the calculation, the mean sizes and rhodium surface atoms were considered.

The number of hydrogen atoms per surface rhodium atoms was calculated taking into account the conversion of norbornene into norbornane, according to literature procedures.^[3] It was assumed the same number of atoms of rhodium in the surface of the nanoparticles due to their similar size. The number of atoms was calculated by the Van Hardevel Hartog that takes into account the structure of the nanoparticles and their diameter.^[4]

General procedure for infrared analysis of rhodium nanoparticles

IR spectroscopy samples were prepared as KBr pellets. The nanoparticles were used without any preparation step, mixed with dry KBr in the glove-box.

General procedure for infrared analysis of rhodium nanoparticles after CO adsorption

For CO coordination studies, rhodium nanoparticles were introduced in a Fischer- Porter bottle and were pressurised with 3 bars of H₂ for 12h to avoid the presence of oxygen on the surface. After this period of time, the dihydrogen gas was evacuated under vacuum for 10 min. The Fischer- Porter bottle was further pressurised with atmosphere CO for 16h. Then, the gas was evacuated under vacuum for 15 min. IR spectroscopy samples were prepared as KBr pellets.

The same procedure was follow for the deuterated experiment, but instead of molecular hydrogen, to avoid the presence of oxygen on the surface, deuterium gas was used.

S2. Synthesis of Rhodium $[\text{Rh}(\eta^3\text{-C}_3\text{H}_5)_3]$ precursor from $\text{RhCl}_3 \cdot 3\text{H}_2\text{O}$

The synthesis was carried out according to the procedure described in the literature.^{[1],[2]}

Allylmagnesium bromide (35mmol) was added to a cold suspension (-10 °C) of $\text{RhCl}_3 \cdot 3\text{H}_2\text{O}$ (1.1 g, 5.3 mmol) in THF (93 ml). The solution slowly lost its red-brown color to become yellow. The solution was then allowed to warm to room temperature and stirred for an additional 16 hours. The solvent was removed under reduced pressure and the residue extracted with pentane (previously distilled and deoxygenated) (3x20 mL). The sublimation was carried out in a water bath at 40 °C and the formation of yellow crystals was observed onto the cold finger. (Yield= 520 mg, 55 %)

S3. Synthesis of rhodium nanoparticles stabilized by P-ligands

The synthesis of the Rh nanoparticles was carried out following the method reported by Chaudret and co-workers.^[3] In a typical procedure, the $[\text{Rh}(\eta^3\text{-C}_3\text{H}_5)_3]$ (64 mg, 0,28 mmol) was placed into a Fischer-Porter reactor and dissolved at -110 °C (acetone/ N_2 bath) in 64 mL of dry and deoxygenated THF (using freeze-pump-thaw techniques) in the presence of the appropriate ligand (0.2 equivalents for bidentate ligands and 0.4 equivalents for monodentate ligands). The Fischer-Porter reactor was then pressurized under 6 bar of H_2 and stirred for 30 minutes at room temperature. The solution was then heated to 40 °C and stirred at this temperature during 24h. The initial colorless solution became black after 1h. A small amount (5 drops approx.) of the solution was deposited under an argon atmosphere on a carbon-covered copper grid for transmission electron microscopy analysis. The rest of the solution was concentrated under reduced pressure. Precipitation and washing with pentane (3 x 15 ml) was then carried out, obtaining a black precipitate. (Yield= *ca.* 25-30 mg, 30-35 %)

S4. Characterization of the rhodium nanoparticles Rh1-Rh2

S4.1 Characterization data for the rhodium nanoparticles Rh1 stabilised by PPh₃ 1

- Nanoparticles **Rh1-0.4**, stabilised by PPh₃ 1

TEM: mean size 1.52 ± 0.21 nm, HRTEM: bond length: 0.26 nm.

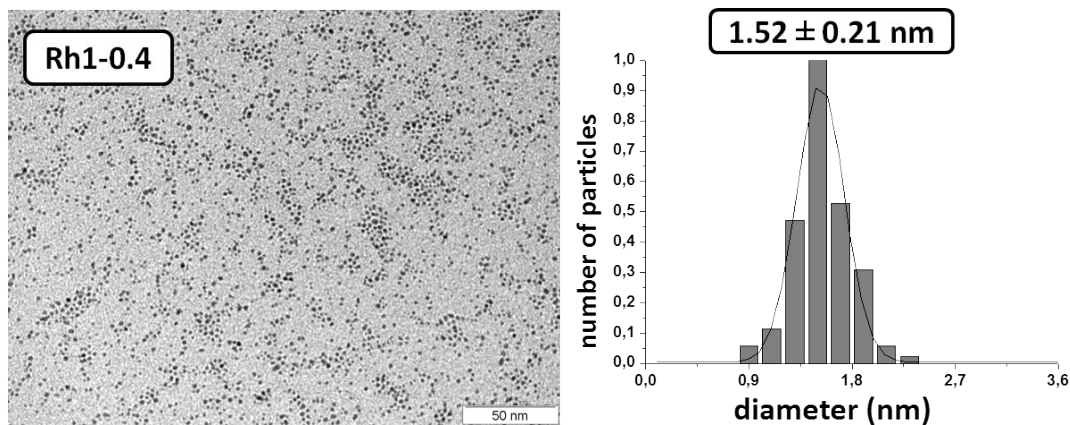


Figure S1 TEM micrograph and size distribution of the **Rh1-0.4** NPs

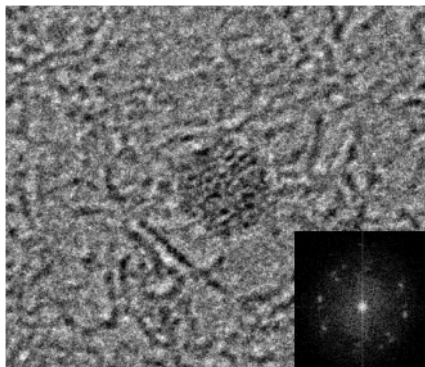


Figure S2 HR-TEM micrograph of **Rh1-0.4**.

XRD: fcc crystalline Rh nanoparticles, coherence length 1.49 ± 0.034

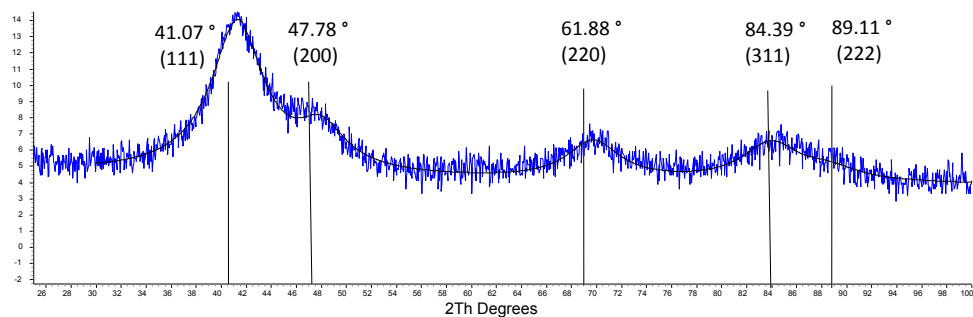


Figure S3 XRD pattern recorded for the nanoparticles **Rh1-0.4**.

WAXS: well-crystallised Rh NPs, coherence length= 2nm, bond length= 0.269nm.

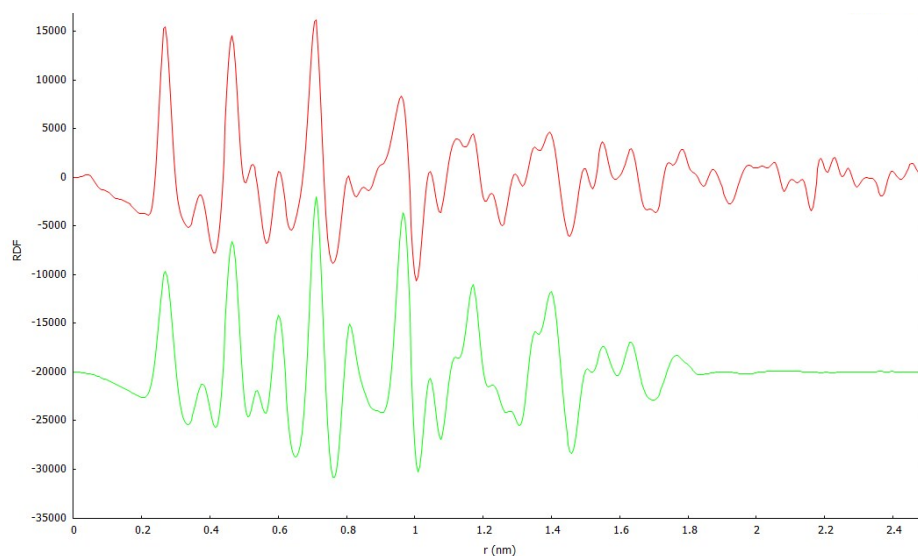


Figure S4 Experimental (red) RDF of **Rh1-0.4** and theoretical (green) RDF for Rh fcc.

XPS: Rh⁰ 3d_{5/2} (308.32eV) 3d_{3/2} (313.02eV) 40% of Rh^{δ+} at the surface of the NPs.

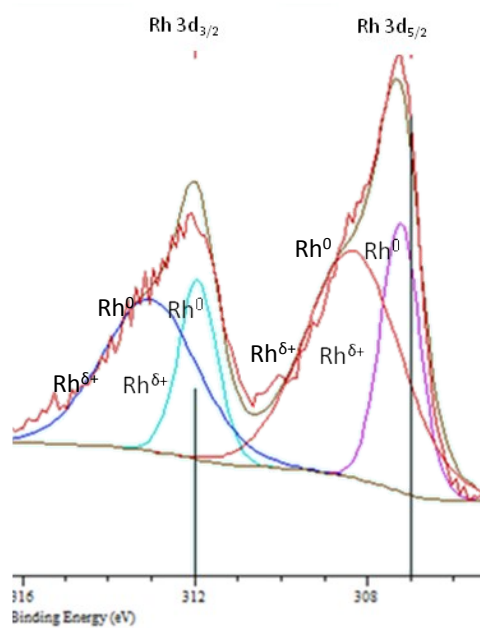


Figure S5 XPS spectra of Rh 3d for nanoparticles **Rh1-0.4**

TGA: 72.1% of Rh, 27.2 % of organic part by TGA

Approximate formula [Rh₁₃₂THF₂L₂₀]

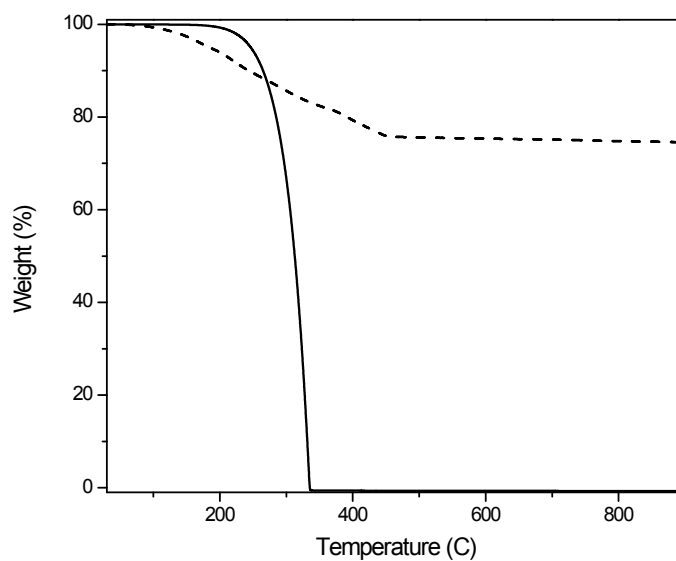


Figure S6 TGA curves of free ligand PPh₃ **1** (solid line) and the corresponding nanoparticle **Rh1-0.4** (dashed line) (10 °C min⁻¹ in N₂).

Hydride titration: 0.8 mol H/ mol of surface Rh

- Nanoparticles **Rh1-0.2**, stabilised by PPh₃ 1

TEM: mean size 1.47 ± 0.28 nm

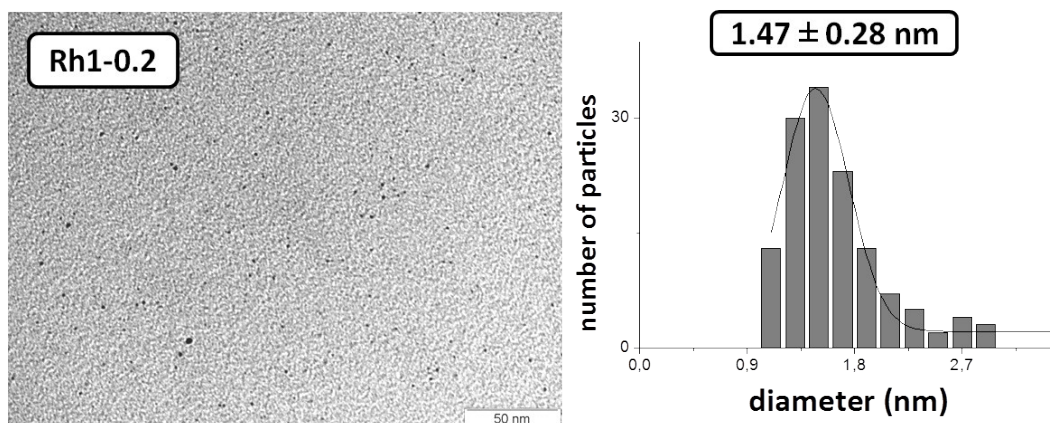


Figure S7 TEM micrograph and size distribution of the **Rh1-0.2** NPs

XRD: fcc crystalline Rh nanoparticles, coherence length 1.39 ± 0.026

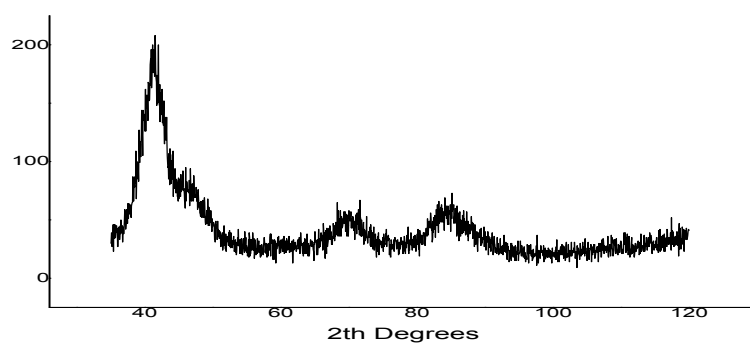


Figure S8 XRD pattern recorded for the nanoparticles **Rh1-0.2**.

XPS: Rh⁰ 3d_{5/2} (307.137eV) 3d_{3/2} (311.903eV), 48% of Rh^{δ+} at the surface of the NPs.

TGA: 55.6% of Rh, 43.8 % of organic part.

Approximate formula $[\text{Rh}_{125}(\text{THF})_2(\text{L})_{39}]$

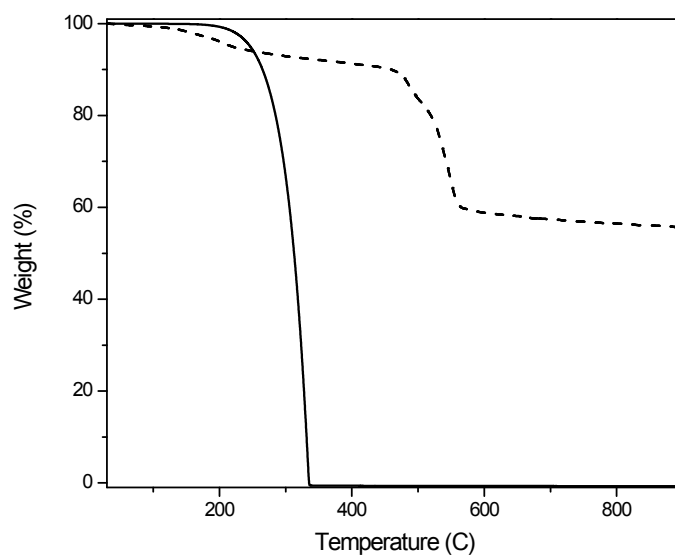


Figure S9 TGA curves of free ligand PPh₃ **1** (solid line) and the corresponding nanoparticle **Rh1-0.2** (dashed line) (10 °C min⁻¹ in N₂).

- Nanoparticles **Rh1-0.6**, stabilised by PPh₃ **1**

TEM: mean size 1.46 ± 0.25 nm

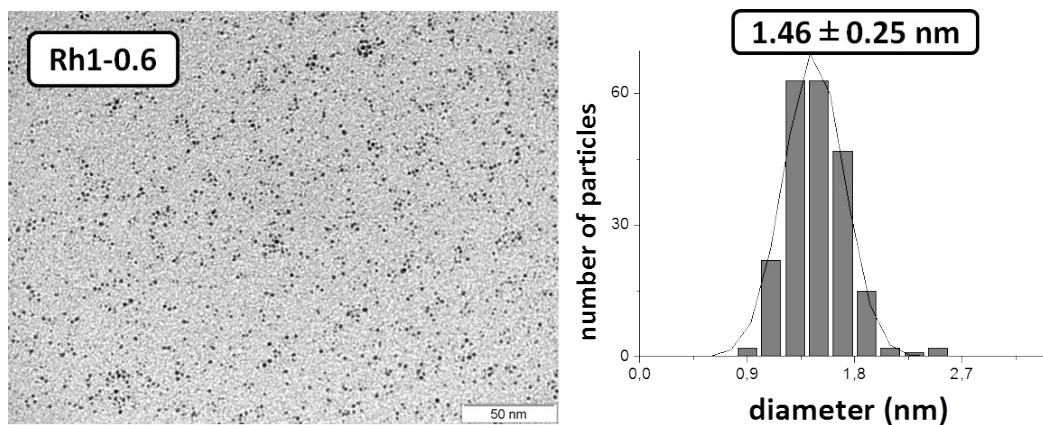


Figure S10 TEM micrograph and size distribution of the **Rh1-0.6** NPs

XRD: fcc crystalline Rh nanoparticles, coherence length 1.46 ± 0.033

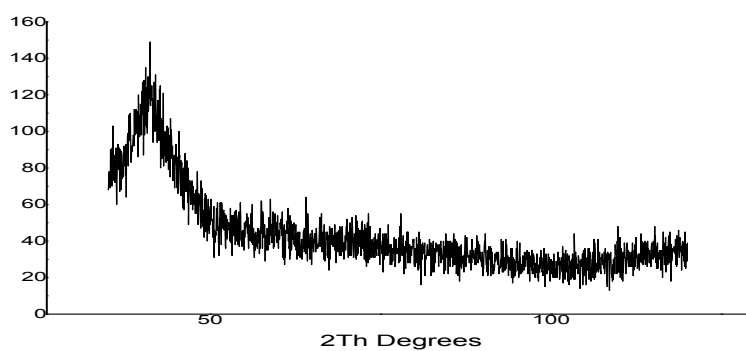


Figure S11 XRD pattern recorded for the nanoparticles **Rh1-0.6**.

XPS: Rh⁰ 3d_{5/2} (307.256eV) 3d_{3/2} (312.129eV) 40% of Rh^{δ+} at the surface of the NPs

TGA: 69.5% of Rh, 29.8 % of organic part

Approximate formula [Rh₁₂₇ THF₂ L₂₁]

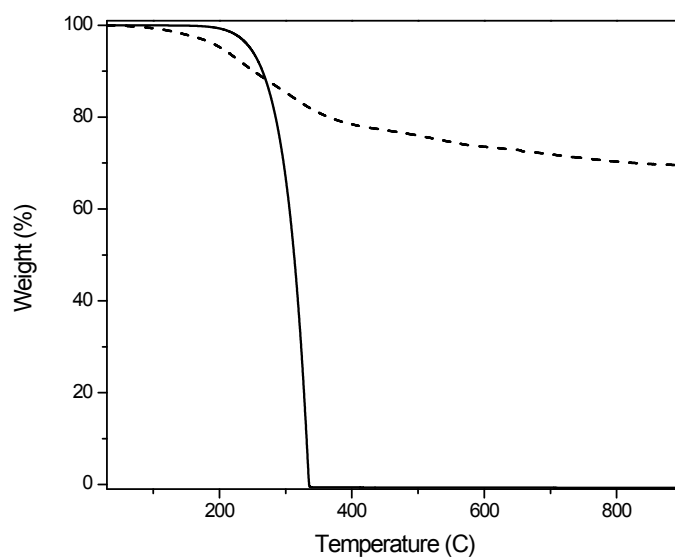


Figure S12 TGA curves of free ligand PPh₃ **1** (solid line) and the corresponding nanoparticle **Rh1-0.6** (dashed line) (10 °C min⁻¹ in N₂).

S4.2 Characterisation data for RhNPs Rh2 stabilised by P(OPh)₃ 2

- Nanoparticles **Rh2-0.4**, stabilised by P(OPh)₃ 2

TEM: mean size 1.52 ± 0.23 nm, HRTEM: bond length: 0.26 nm.

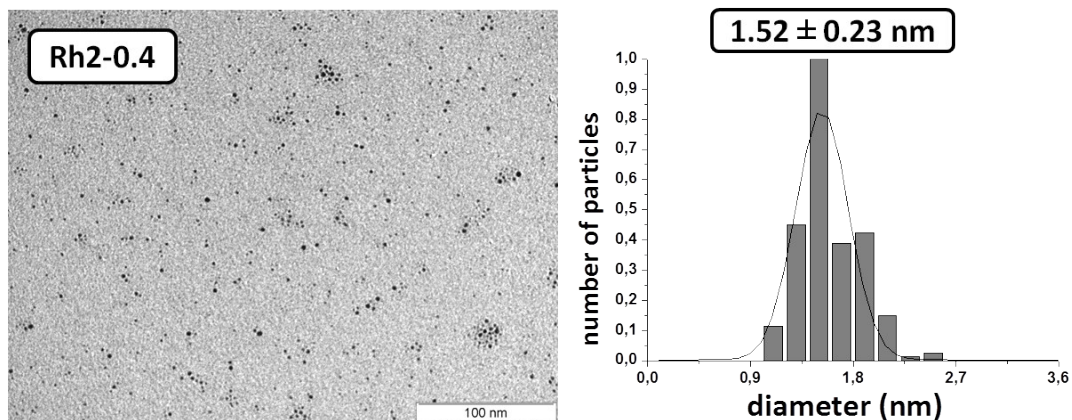


Figure S13 TEM micrograph and size distribution of the **Rh2-0.4** NPs

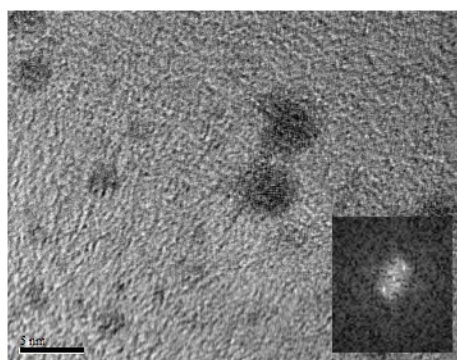


Figure S14 HRTEM image of **Rh2-0.4** NPs.

XRD: fcc crystalline Rh nanoparticles, coherence length 1.53 ± 0.023 nm

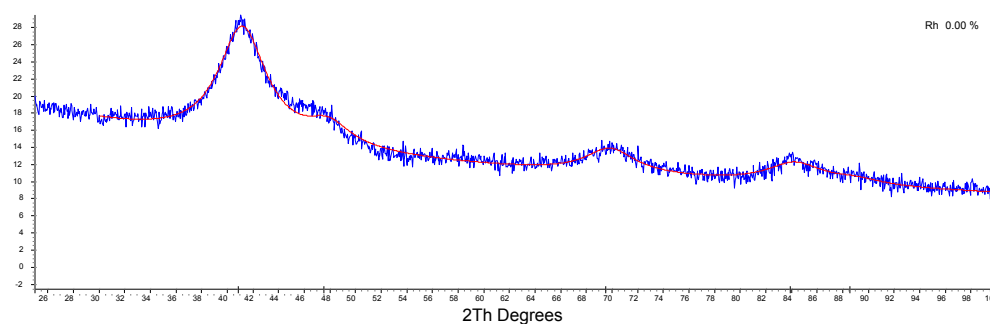


Figure S15 XRD pattern recorded for the nanoparticles **Rh2-0.4**.

XPS: Rh⁰ 3d5/2 (308.0eV) 3d3/2 (312.77eV) Rh⁰ at the surface of the NPs

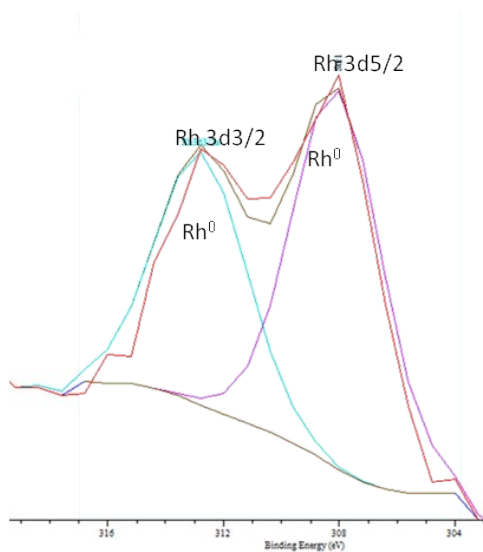


Figure S16 XPS spectra of Rh 3d for nanoparticles **Rh2-0.4**.

TGA: 58% of Rh, 40.3 % of organic part

Approximate formula [Rh₁₃₂ THF₆ L₃₀]

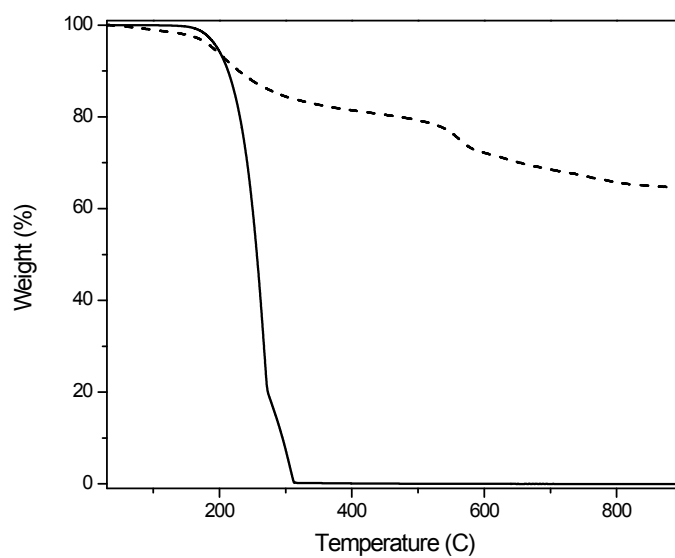


Figure S17 TGA curves of free ligand P(OPh)₃ **2** (solid line) and the corresponding nanoparticle **Rh2-0.4** (dashed line) (10 °C min⁻¹ in N₂)

Hydride titration: 0.3 mol H / mol surface Rh

- Nanoparticles **Rh2-0.1**, stabilised by P(OPh)_3 2

TEM: mean size $1.57 \pm 0.23 \text{ nm}$

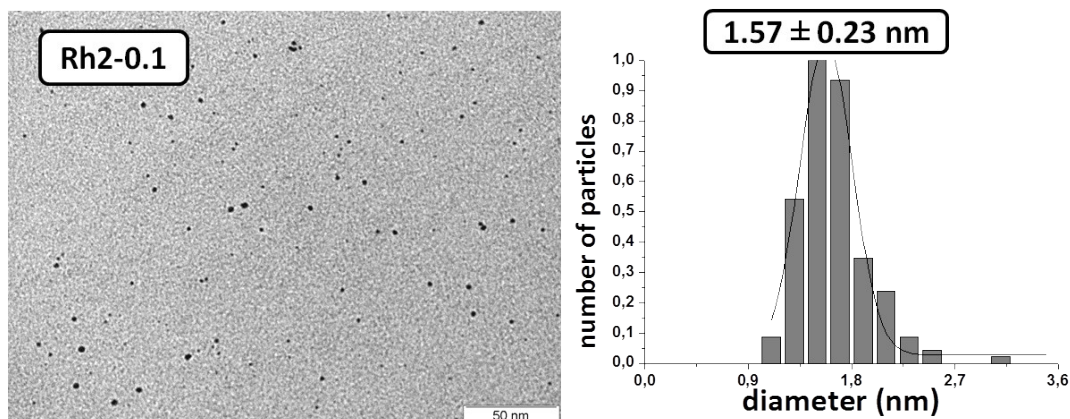


Figure S18 TEM micrograph and size distribution of the **Rh2-0.1** NPs

XRD: fcc crystalline Rh nanoparticles, coherence length $1.53 \pm 0.04 \text{ nm}$

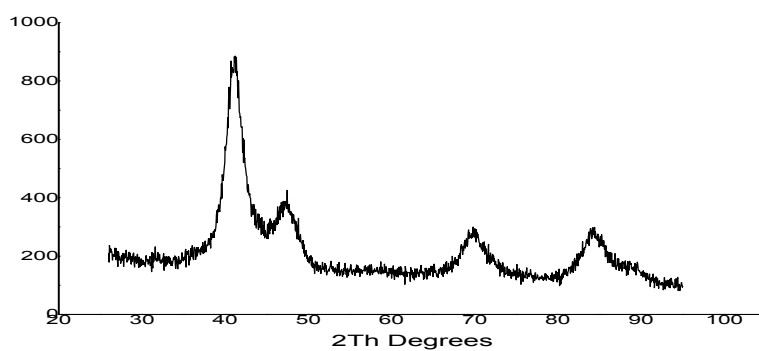


Figure S19 XRD pattern recorded for the nanoparticles **Rh2-0.1**.

XPS: Rh^0 3d5/2 (307.5eV) 3d3/2 (311.8eV) 40% of $\text{Rh}^{\delta+}$ at the surface of the NPs

TGA: 64.5% of Rh, 33.7 % of organic part

Approximate formula [Rh₁₄₆ THF₈ L₂₅]

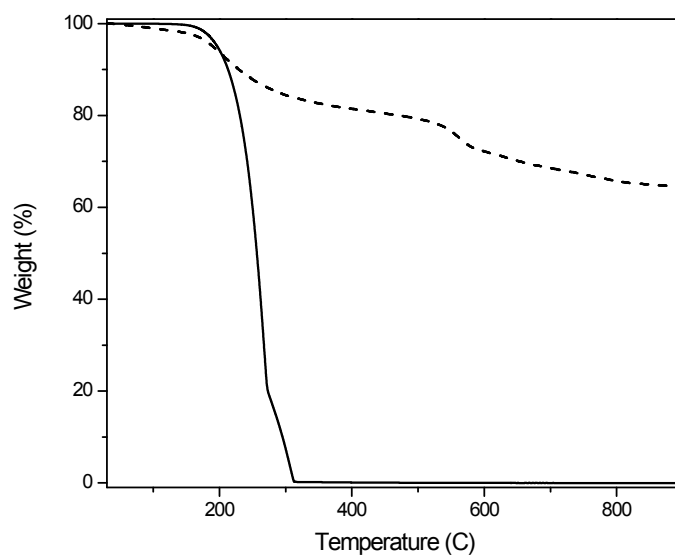


Figure S20 TGA curves of free ligand P(OPh)₃ **2** (solid line) and the corresponding nanoparticle **Rh2-0.1** (dashed line) (10 °C min⁻¹ in N₂)

- Nanoparticles **Rh2-0.2**, stabilised by $P(OPh)_3$ 2

TEM: mean size 1.55 ± 0.31 nm

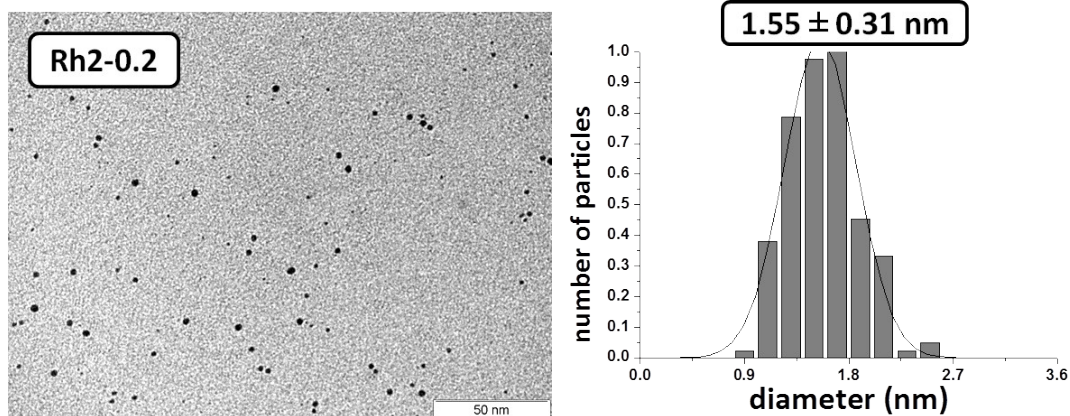


Figure S21 TEM micrograph and size distribution of the **Rh2-0.2** NPs

XRD: fcc crystalline Rh nanoparticles, coherence length 1.64 ± 0.05 nm

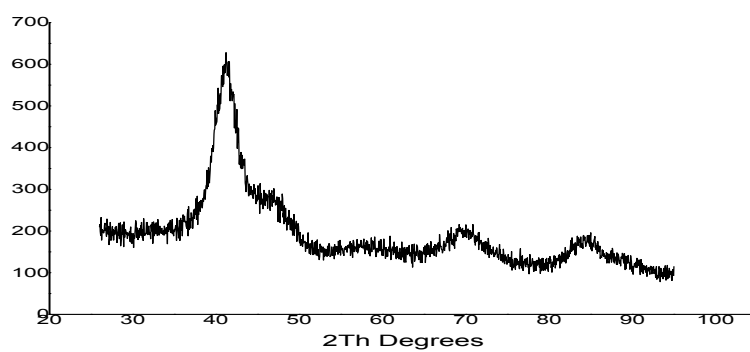


Figure S22 XRD pattern recorded for the nanoparticles **Rh2-0.2**.

XPS: Rh^0 3d5/2 (307.9eV) 3d3/2 (312.4eV) 40% of $Rh^{\delta+}$ at the surface of the NPs

TGA: 62.3% of Rh, 35.7 % of organic part

Approximate formula $[Rh_{140} THF_3 L_{11}]$

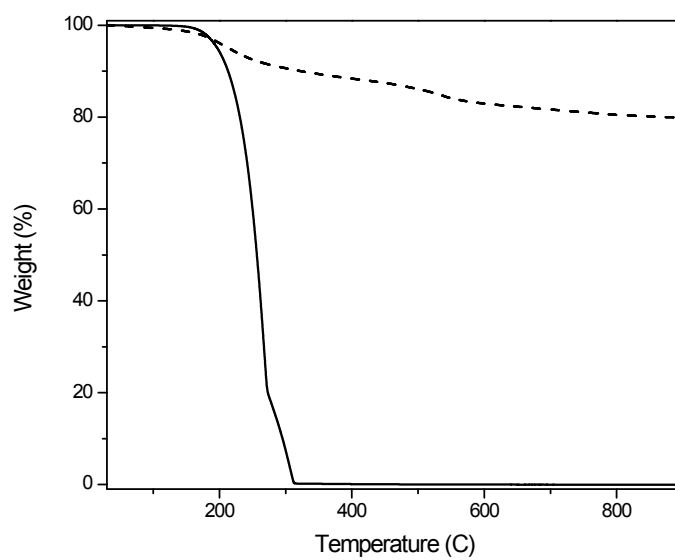


Figure S23 TGA curves of free ligand P(OPh)₃ 2 (solid line) and the corresponding nanoparticle **Rh2-0.2** (dashed line) (10 °C min⁻¹ in N₂)

- Nanoparticles **Rh2-0.6**, stabilised by $P(O\text{Ph})_3$ **2**

TEM: mean size 1.65 ± 0.30 nm

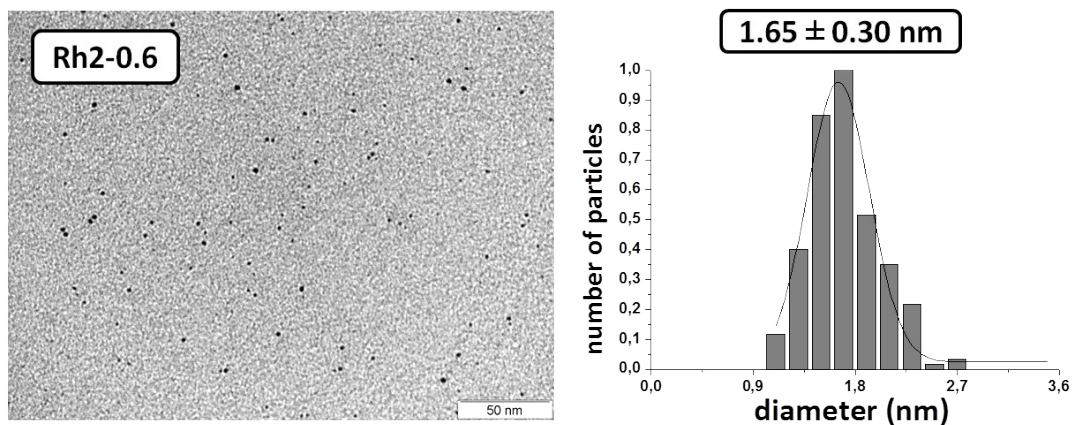


Figure S24 TEM micrograph and size distribution of the **Rh2-0.6** NPs

XRD: fcc crystalline Rh nanoparticles, coherence length 1.53 ± 0.04 nm

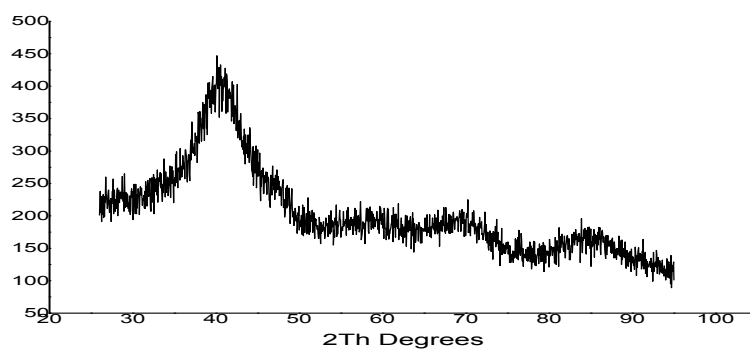


Figure S25 XRD pattern recorded for the nanoparticles **Rh2-0.6**.

XPS: Rh^0 3d5/2 (307.561eV) 3d3/2 (312.546eV) 40% of $\text{Rh}^{\delta+}$ at the surface of the NPs

TGA: 45.3% of Rh, 53.4 % of organic part

Approximate formula [Rh₁₆₉ THF₉ L₆₆]

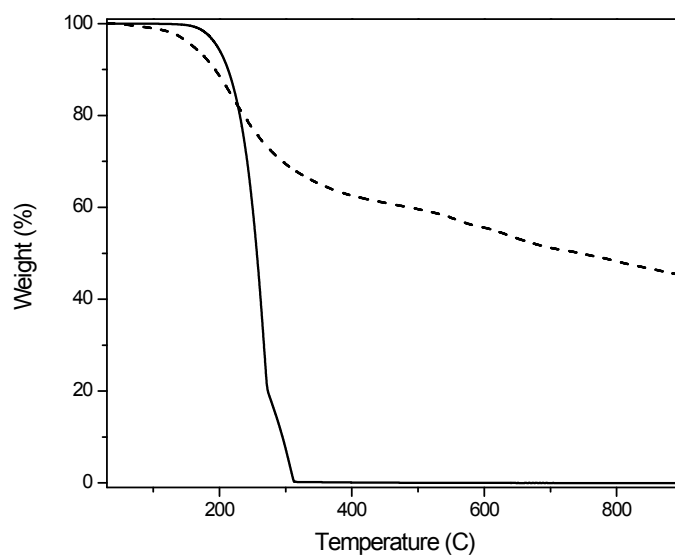


Figure S26 TGA curves of free ligand P(OPh)₃ **2** (solid line) and the corresponding nanoparticle **Rh2-0.6** (dashed line) (10 °C min⁻¹ in N₂)

S4.3 Solution NMR spectra

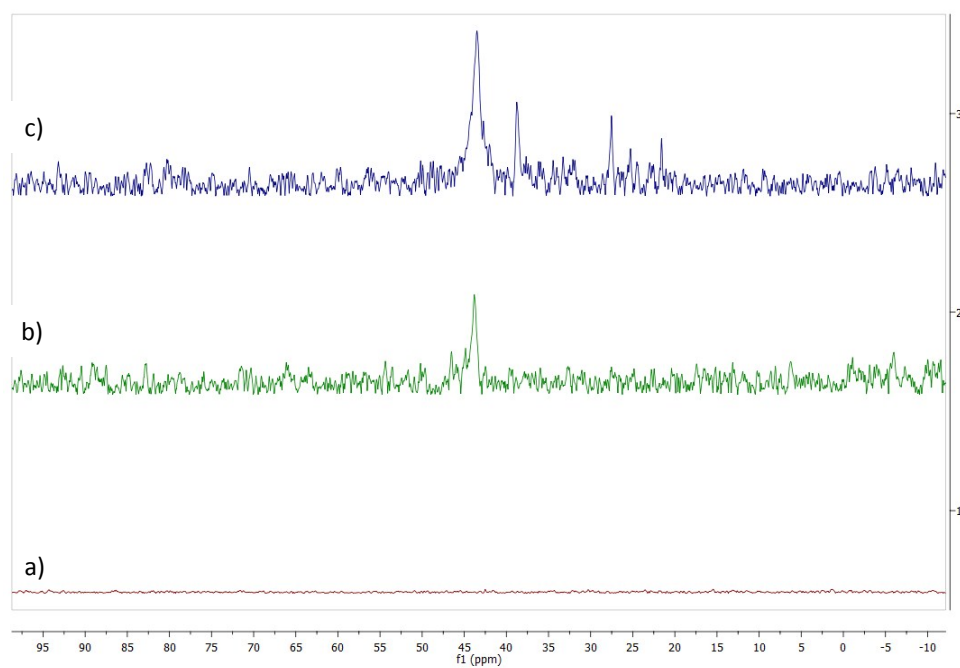


Figure S27 Solution $^{31}\text{P}\{\text{H}\}$ NMR spectra of Rh1-0.4 NPs at a) room temperature, b) -80 °C, c) room temperature under 30 bar of CO pressure.

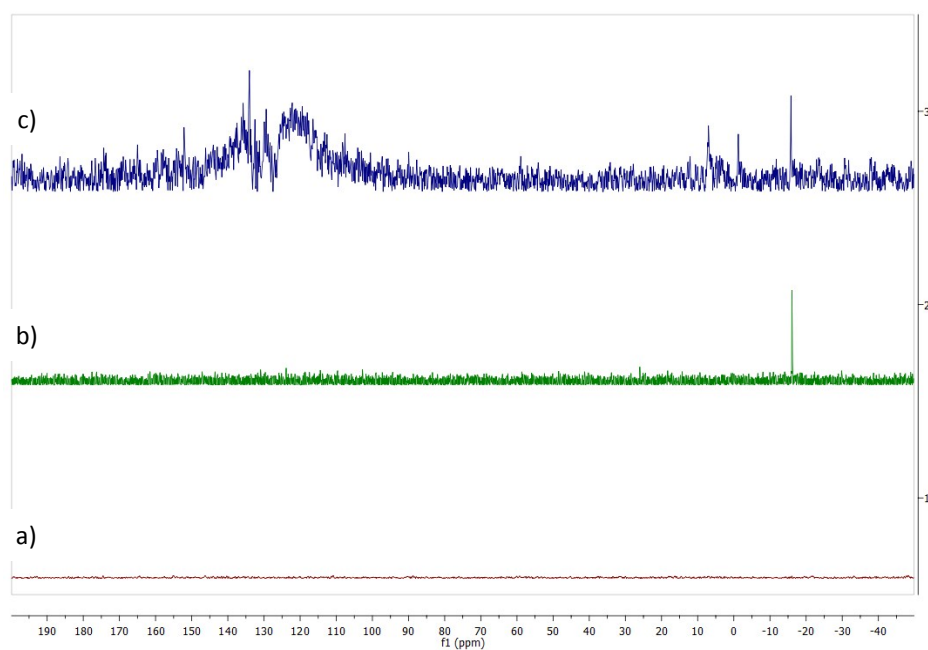


Figure S28 Solution $^{31}\text{P}\{\text{H}\}$ NMR spectra of Rh-NPs Rh2-0.4 in $d_8\text{THF}$ at a) room temperature, b) -80 °C, c) after 30 bar of CO pressure.

S4.4 FTIR spectra

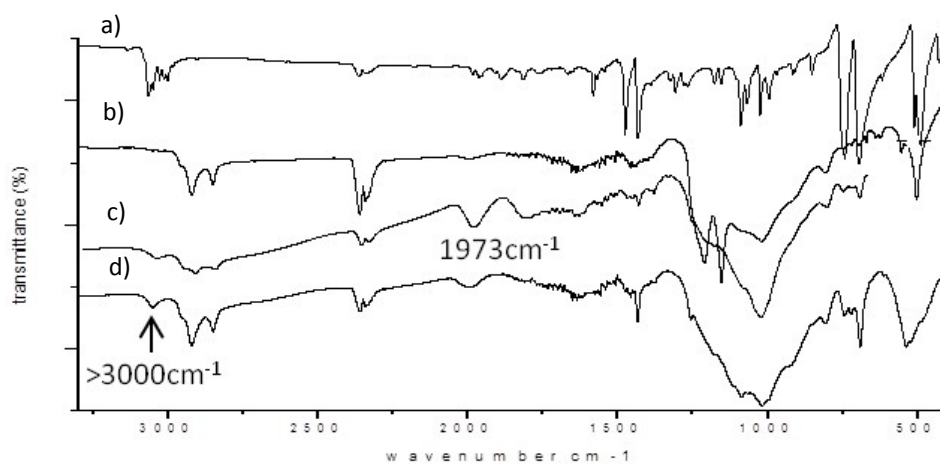


Figure S29 IR spectra of: a) PPh_3 1, b) Rh1-0.2, c) Rh1-0.4, d) Rh1-0.6 NPs.

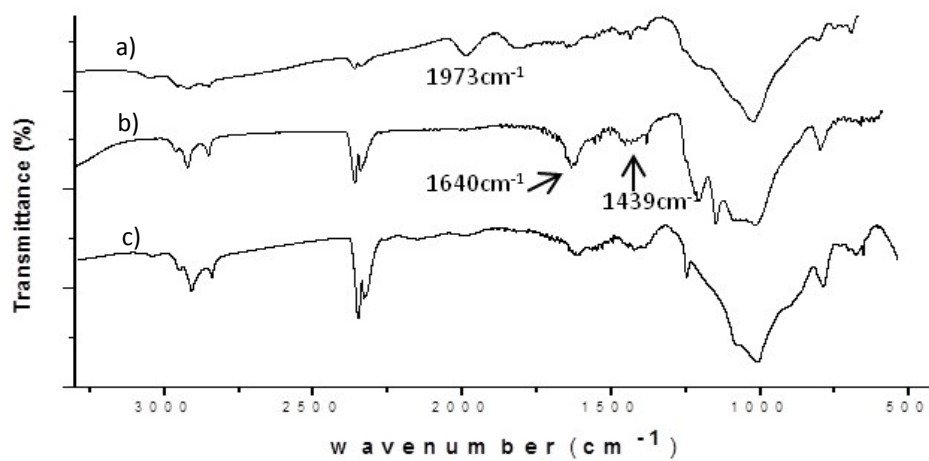


Figure S30 IR spectra of a) Rh1-0.4; b) Rh1-0.4 after titration with norbornene; c) Rh1-0.4-D2.

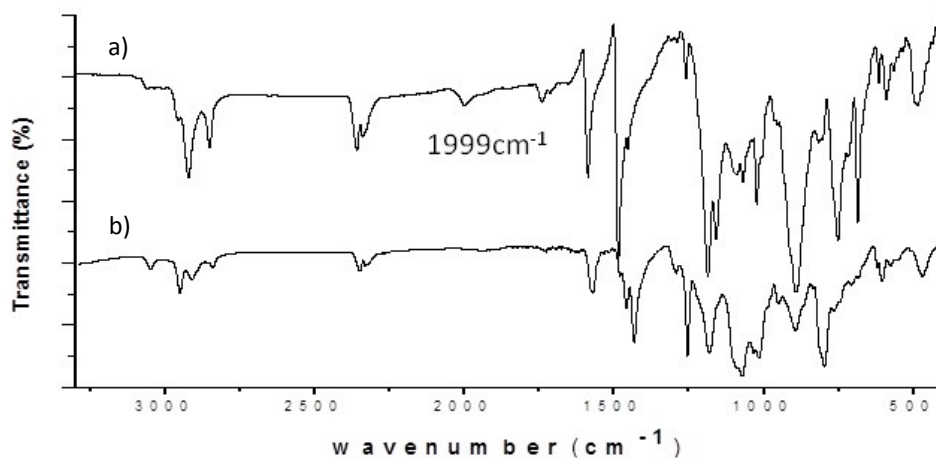


Figure S31 IR spectra of a) Rh2-0.4 NPs b) Rh2-0.4 D₂ NPs.

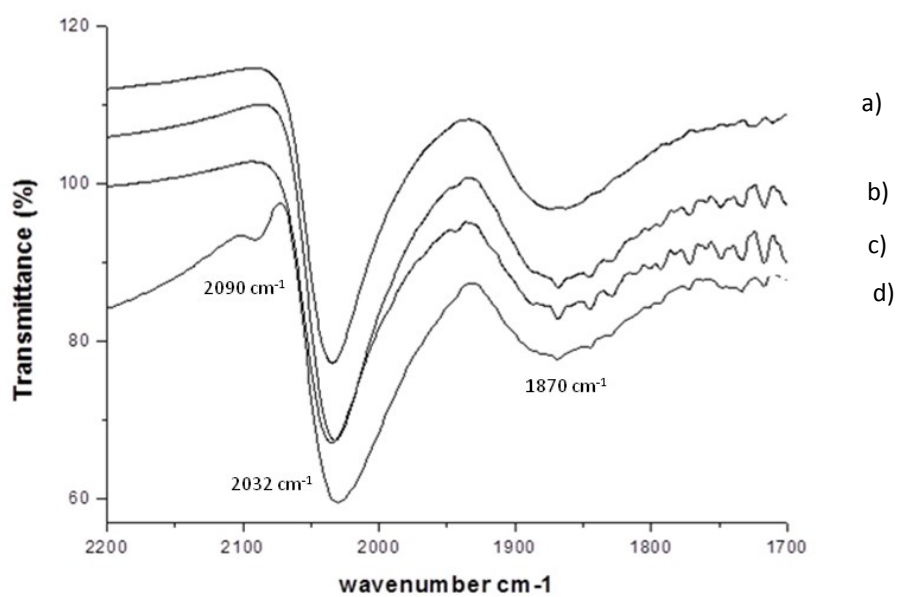


Figure S32 Carbonyl region of the IR spectra of Rh1-0.4 NPs under CO atmosphere after a) 2h, b) 4h, c) 6h and d) 12h.

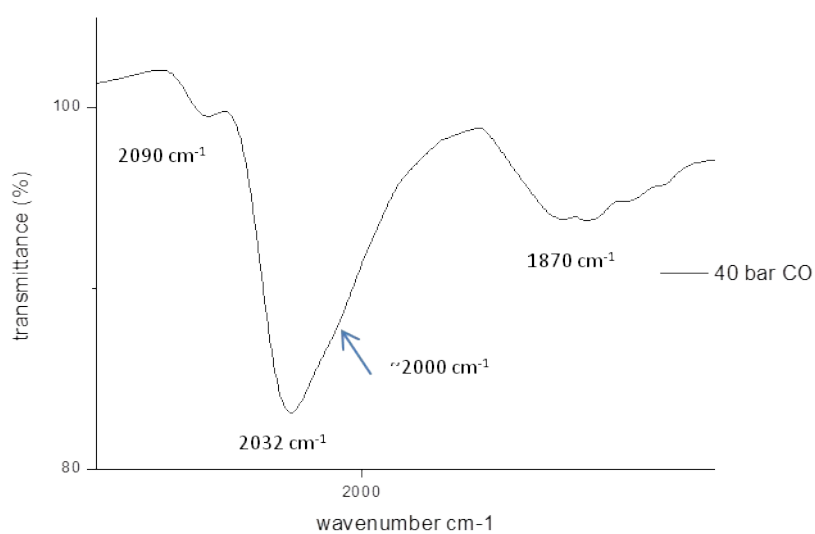


Figure S33 Carbonyl region of the IR spectra of **Rh1-0.4** NPs after exposition to 40 bar of CO pressure.

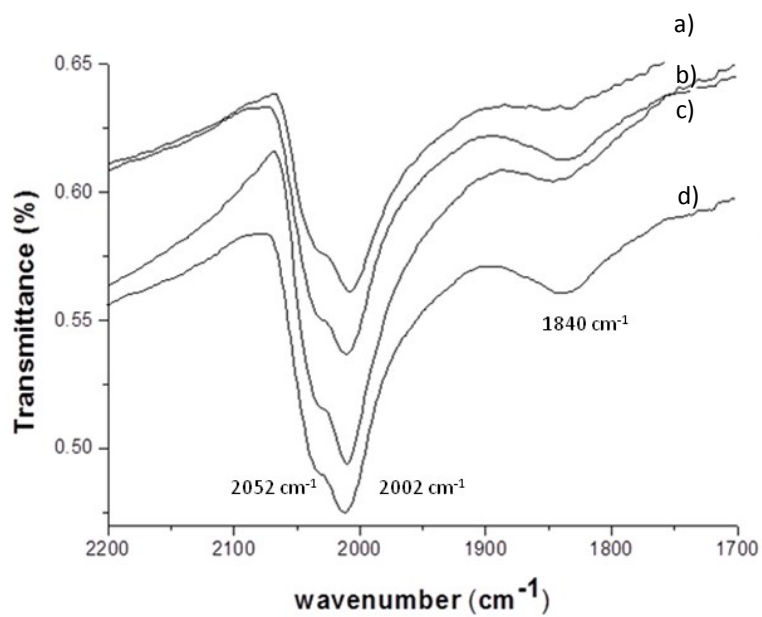


Figure S34 Carbonyl region of IR spectra of **Rh2-0.4** NPs after CO adsorption during a) 2h, b) 4h, c) 6h and d) 12h.

S5. References

- [1] M. D. Fryzuk, W. E. Piers in *Organometallic Syntheses* (Eds.:R. B. King, J. J. Eisch), Elsevier, Amsterdam, **1986**, vol. 3, p.128.
- [2] W. A. Herrmann in *Synthetic Methods of Organometallic and Inorganic Chemistry* (Ed.: W. A. Herrmann), Thieme, Stuttgart, **1996**, p. 38.
- [3] J. García-Antón, M. R. Axet, S. Jansat, K. Philippot, B. Chaudret, T. Pery, G. Buntkowsky, H.-H. Limbach *Angew. Chem. Int. Ed.* **2008**, *47*, 2074-2078.
- [4] V. Hardevel, V. Hartog, *Surf. Sci.* **1969**, *15*, 189-230, A. Borodzinski, M. Bonarowska, *Langmuir*, **1997**, *13*, 5613-5620.